Supplementary information

Constraining the Effects of Anthropogenic Emissions and Meteorological Variabilities on summertime $PM_{2.5}$ and surface ozone changes over eastern China during 2015-2024

Ganquan Zeng et al.

Correspondence to: Xiao Lu (luxiao25@mail.sysu.edu.cn)

Table S1. List of cities used in the study and the number of stations in each city.

Region	City
NCP (207)	Beijing (12), Tianjin (14), Shijiazhuang (7), Tangshan (6), Qinhuangdao (5), Baoding (6), Zhangjiakou (5), Chengde (5), Langfang (4), Cangzhou (3), Hengshui (3), Handan (4), Xingtai (4), Jinan (8), Qingdao (9), Laiwu (3), Linyi (4), Dezhou (3), Liaocheng (3), Binzhou (3), Zibo (6), Zaozhuang (5), Weifang (5), Tai'an (3), Jining (3), Rizhao (3), Dongying (4), Heze (3), Zhengzhou (9), Anyang (5), Hebi (3), Jiaozuo (4), Kaifeng (4), Luohe (4), Nanyang (5), Pingdingshan (4), Puyang (4), Shangqiu (4), Xinxiang (4), Xinyang (4), Xuchang (3), Zhoukou (4), Zhumadian (3)
YRD (191)	Shanghai (9), Nanjing (9), Suzhou (Jiangsu) (8), Nantong (5), Lianyungang (4), Xuzhou (7), Yangzhou (4), Wuxi (8), Changzhou (6), Zhenjiang (3), Taizhou (Jiangsu) (4), Huai'an (5), Yancheng (4), Suqian (4), Hangzhou (11), Ningbo (7), Wenzhou (4), Shaoxing (3), Huzhou (3), Jiaxing (2), Taizhou (Zhejiang) (3), Zhoushan (3), Jinhua (3), Quzhou (3), Lishui (3), Hefei (10), Anqing (4), Bengbu (6), Chizhou (3), Chuzhou (3), Fuyang (2), Huaibei (3), Huainan (5), Huangshan (3), Lu'an (4), Ma'anshan (5), Suzhou (Anhui) (3), Tongling (6), Wuhu (4), Xuancheng (3), Bozhou (2)

Table S2. WRF-CMAQ configurations.

Category	Configuration
Model version	WRF, version 4.2; CMAQ, version 5.5
Model domain	Covers all of China (Fig. 2a)
Grid resolution	27 km × 27 km
Vertical layers	35 layers from surface to 100 hPa
Microphysics	Purdue Lin scheme (Chen and Sun, 2002)
Longwave radiation	Rapid Radiative Transfer Model (Mlawer et al., 1997)
Shortwave radiation	Goddard (Chou et al., 2001)
Boundary layer	the Yonsei University scheme (Hong et al., 2006)
Surface physics	Unified Noah land-surface model
Biogenic emissions	Calculated online using MEGAN in CMAQ
Photolysis	CMAQ inline photolysis module
Gas phase chemistry	Carbon Bond 6 Revision 5 mechanism (CB6R5)
Aerosols	CMAQ AERO7 aerosol module

Table S3. Meteorological observation sites used to evaluate WRF output.

Region	Province	Site ID
NCP	Beijing	545110
	Tianjin	545270, 545273
	Hebei	535930, 537980, 543080, 543110, 544010, 544050, 544230, 544360, 545340, 545390, 546020, 546180
	Henan	538980, 570710, 570830, 571780, 571930, 572900, 572970, 582080
	Shandong	547150, 547250, 547510, 547530, 547760, 548080, 548230, 548260, 548360, 548430, 548570, 548630, 549090, 549160, 549290, 549450
YRD	Shanghai	583620, 583670
	Anhui	581020, 582030, 582210, 583410, 583210, 583211, 583380, 584370
	Jiangsu	580270, 580400, 581410, 581500, 582380, 582510, 582650, 583450
	Zhejiang	584570, 584720, 584770, 585430, 585560, 585690, 586460, 586590, 586660, 587520

Table S4. Statistical evaluation of WRF-simulated surface meteorological variables over EACN, NCP, and YRD during 2015-2019.

Variables	Metrics	EACN	NCP	YRD
2m T (°C)	Observation (mean)	26.52	25.86	27.34
	Simulation (mean)	26.91	26.91	27.00
	MB	0.43	1.05	-0.34
	RMSE	3.65	3.85	3.38
	r	0.76	0.79	0.74
	IOA	0.86	0.87	0.85
2m RH (%)	Observation (mean)	74.85	71.03	79.57
	Simulation (mean)	61.64	54.40	70.60
	MB	-13.20	-16.62	-8.97
	RMSE	19.92	22.58	16.03
	r	0.76	0.75	0.73
	IOA	0.79	0.77	0.80
SLP (hPa)	Observation (mean)	1005.41	1005.27	1005.62
	Simulation (mean)	1005.81	1005.66	1006.04
	MB	0.40	0.39	0.42
	RMSE	1.07	1.17	0.91
	r	0.97	0.96	0.98
	IOA	0.98	0.98	0.98
10m WS (m s^{-1})	Observation (mean)	2.79	2.58	3.04
	Simulation (mean)	3.40	3.36	3.44
	MB	0.61	0.78	0.40
	RMSE	1.83	1.89	1.75
	r	0.54	0.48	0.62
	IOA	0.72	0.65	0.77

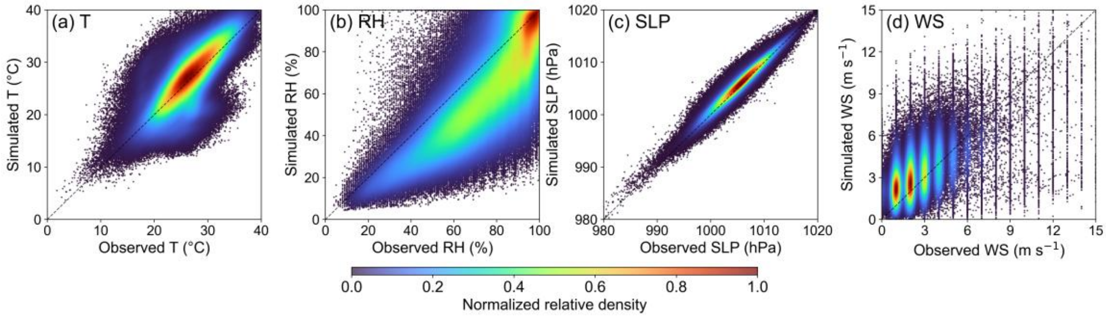

Figure S1. Scatter plots comparing observed (horizontal axis) and WRF-simulated (vertical axis) meteorological parameters during the 2015-2019 simulations: (a) 2 m temperature (T), (b) 2 m relative humidity (RH), (c) sea level pressure (SLP), (d) 10 m wind speed (WS).

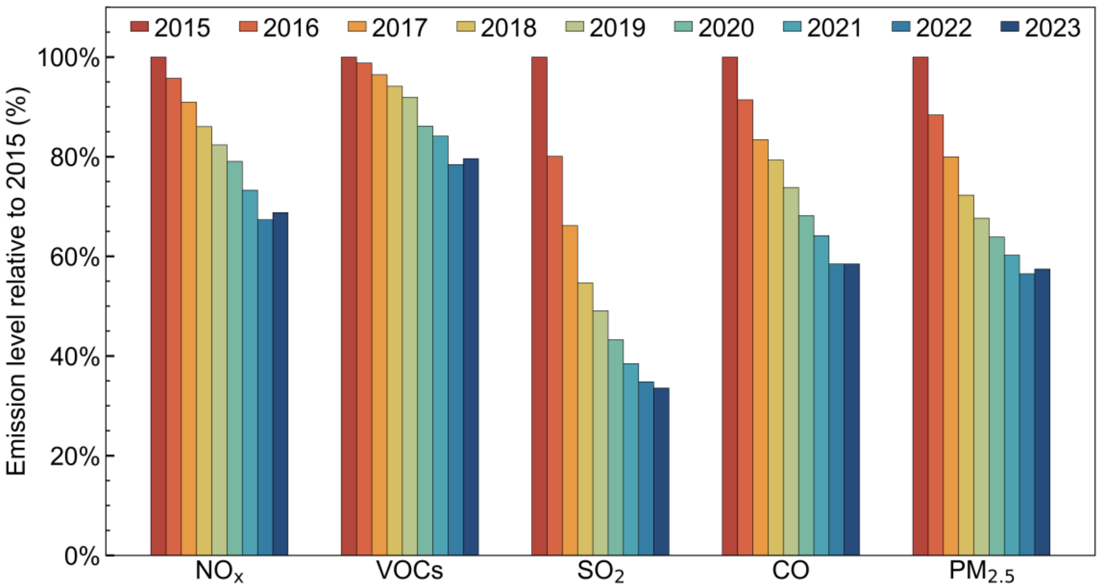

Figure S2. Relative changes in anthropogenic emissions of NO_x, VOCs, SO_2, CO, and primary $PM_{2.5}$ over EACN from the MEIC v2.0 inventory during 2015-2023. Values are normalized to 2015 levels, with 2015 set to 100%.

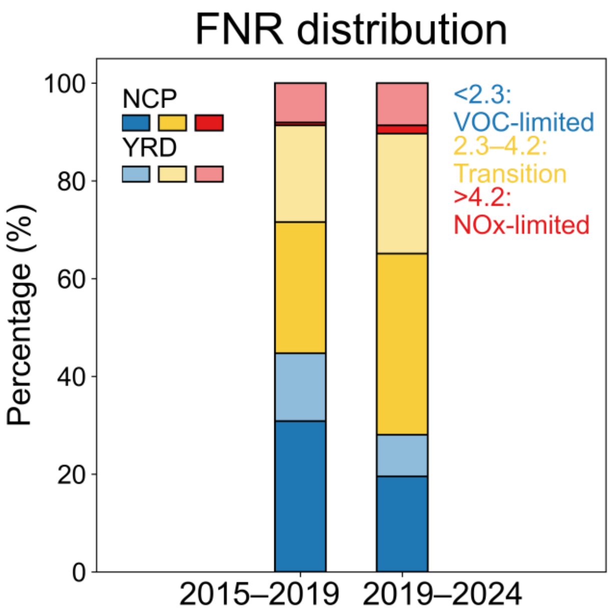

Figure S3. Distribution of summertime ozone sensitivity regimes over eastern China during 2015-2024. The panel shows the fractional coverage of ozone sensitivity regimes in eastern China for the periods 2015-2019 and 2019-2024. Blue, yellow, and red denote VOC-limited, transitional, and NO_x-limited regimes, respectively. Color shading (light vs. dark) further distinguishes the North China Plain (NCP) and the Yangtze River Delta (YRD).

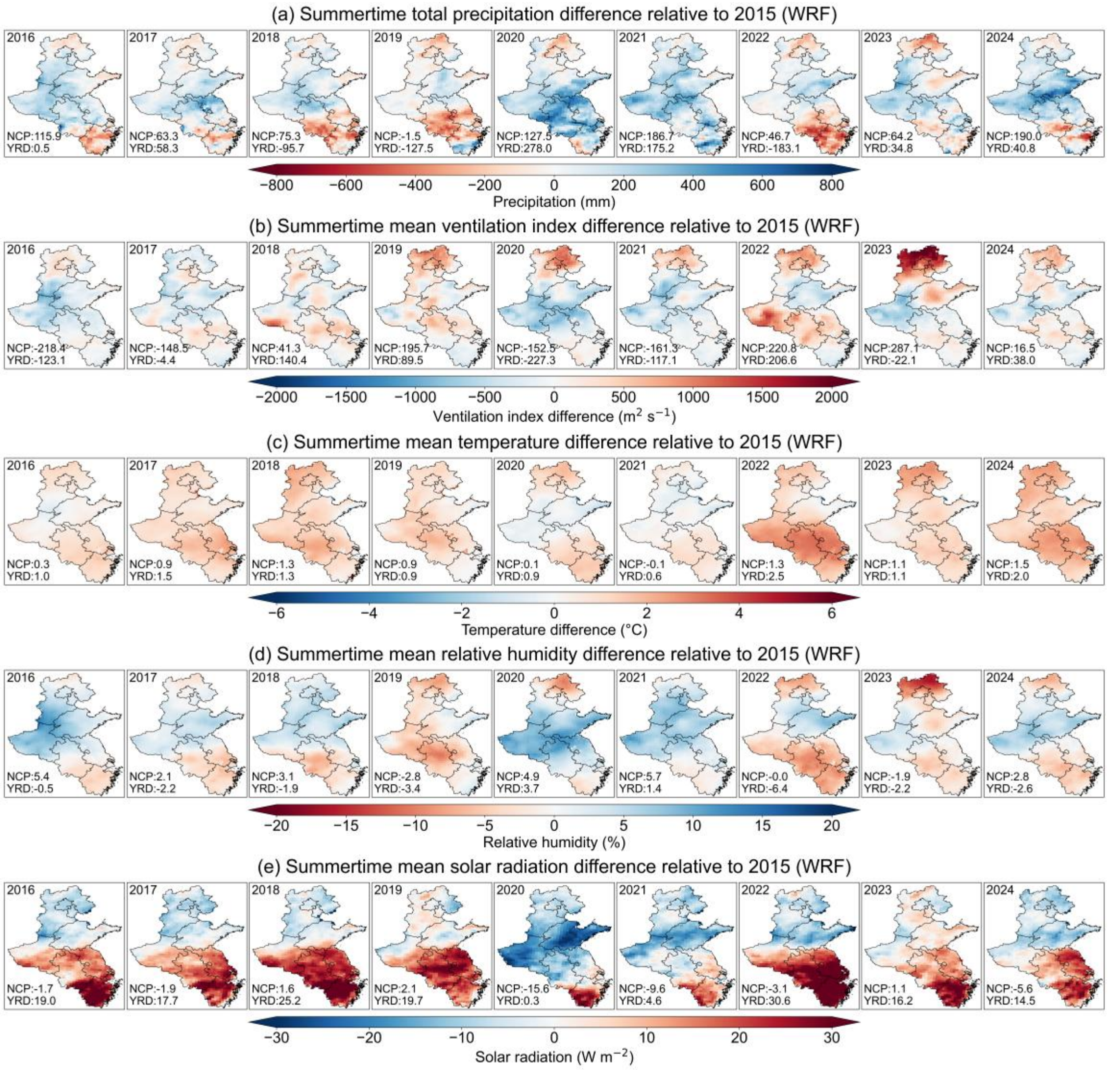

Figure S4. Interannual variations in summertime meteorological factors from 2016 to 2024 relative to 2015 levels simulated by WRF, including (a) total precipitation difference, (b) mean ventilation index difference, (c) mean 2-meter temperature difference, (d) mean relative humidity difference, and (e) mean solar radiation difference.

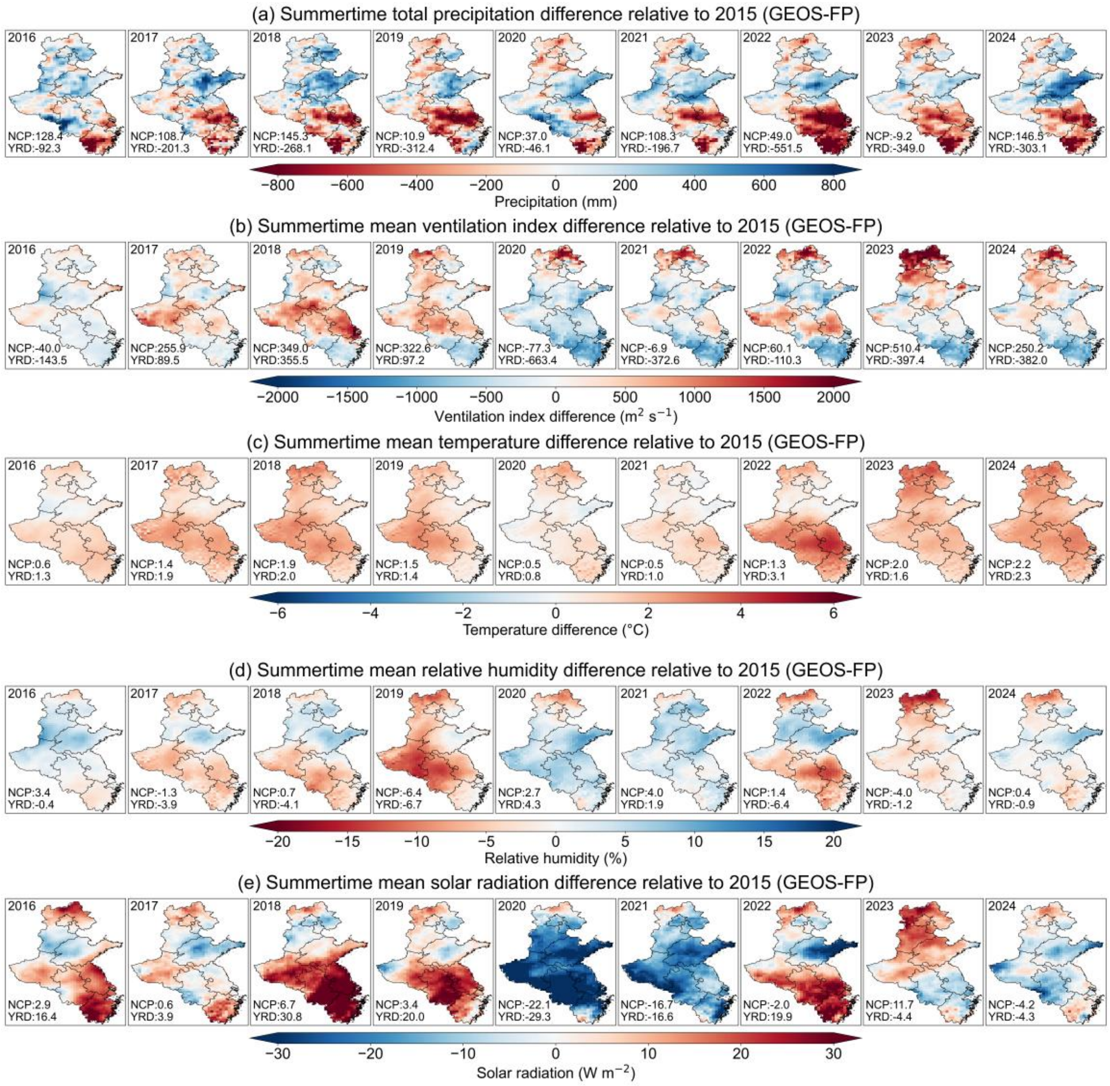

Figure S5. Same as Figure S4, but for the GEOS-FP meteorological fields used to drive the GEOS-Chem simulations.

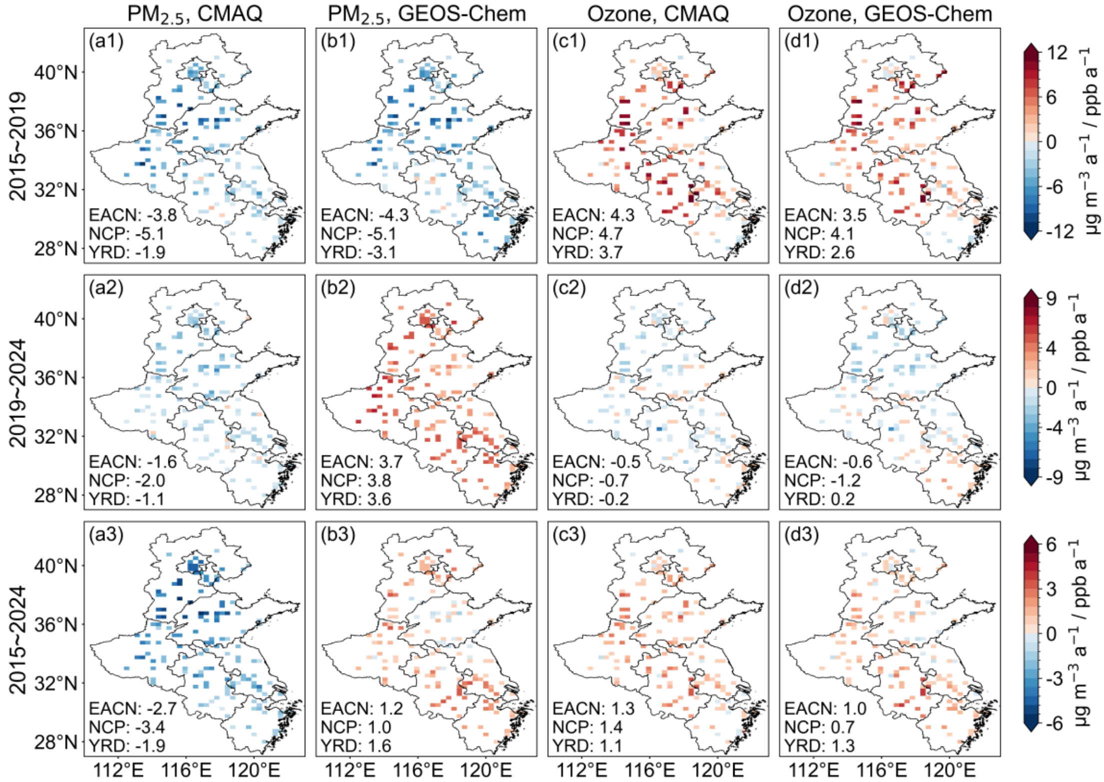

Figure S6. Spatial distribution of anthropogenic emission-driven changes in summertime surface daily $PM_{2.5}$ and ozone concentrations over eastern China during three periods (2015-2019, 2019-2024, and 2015-2024) as attributed by CMAQ and GEOS-Chem. Panels (a, b) show the emission-driven contributions to $PM_{2.5}$ changes derived from CMAQ and GEOS-Chem, respectively. Panels (c, d) show the same but for ozone. Trends at each grid cell are calculated based on monthly mean daily $PM_{2.5}$ and MDA8 ozone concentration anomalies defined as the deviation of the monthly mean from the multi-year average of the corresponding calendar month over 2015-2024.

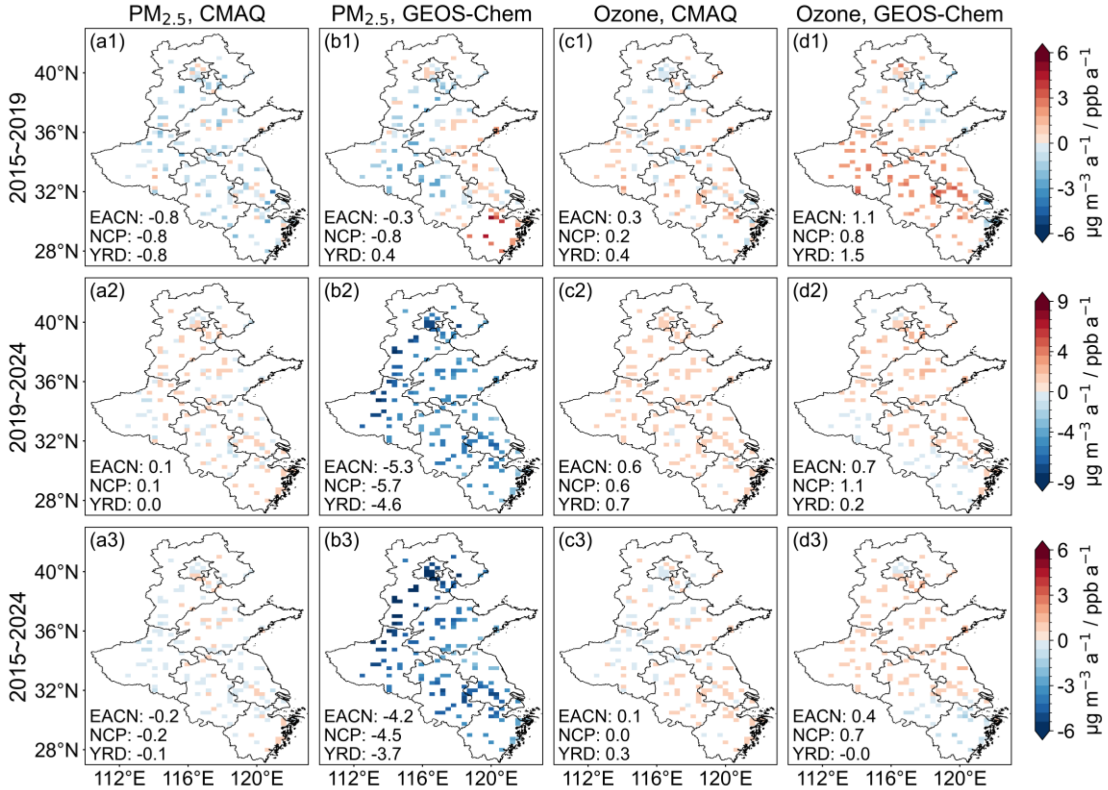

Figure S7. Same as Figure S6 but for meteorology-driven changes in daily $PM_{2.5}$ and MDA8 ozone.

References

Chen, S.-H. and Sun, W.-Y.: A One-dimensional Time Dependent Cloud Model, Journal of the Meteorological Society of Japan. Ser. II, 80, 99-118, https://doi.org/10.2151/jmsj.80.99, 2002.

Chou, M.-D., Suarez, M. J., Liang, X.-Z., Yan, M. M. H., and Cote, C.: A Thermal Infrared Radiation Parameterization for Atmospheric Studies, NASA Goddard Space Flight Center, Greenbelt, MDNASA/TM-2001-104606/VOL19, https://ntrs.nasa.gov/citations/20010072848, 2001.

Hong, S. Y., Noh, Y., and Dudhia, J.: A new vertical diffusion package with an explicit treatment of entrainment processes, Monthly Weather Review, 134, 2318-2341, https://doi.org/10.1175/MWR3199.1, 2006.

Mlawer, E. J., Taubman, S. J., Brown, P. D., Iacono, M. J., and Clough, S. A.: Radiative transfer for inhomogeneous atmospheres: RRTM, a validated correlated-k model for the longwave, Journal of Geophysical Research: Atmospheres, 102, 16663-16682, https://doi.org/10.1029/97jd00237, 1997.